



Contents lists available at ScienceDirect

## Arabian Journal of Chemistry

journal homepage: [www.ksu.edu.sa](http://www.ksu.edu.sa)

# Evaluation of slow-release fertilizers derived from hydrogel beads: Sodium alginate-poly (acrylic acid) and humic acid-encapsulated struvite for soil salinity amelioration

Endar Hidayat<sup>a,b,c</sup>, Nur Maisarah Mohamad Sarbani<sup>a,b</sup>, Sadaki Samitsu<sup>c</sup>,  
Ferry Anggoro Ardy Nugroho<sup>d</sup>, Sudip Kumar Lahiri<sup>e,f</sup>, Mitsuru Aoyagi<sup>a,b</sup>,  
Seiichiro Yonemura<sup>a,b</sup>, Hiroyuki Harada<sup>a,b,\*</sup>

<sup>a</sup> Graduate School of Comprehensive Scientific Research, Program in Biological System Sciences, Prefectural University of Hiroshima, Shobara 727-0023, Japan

<sup>b</sup> Department of Life System Science, Faculty of Bioresources Science, Prefectural University of Hiroshima, Shobara 727-0023, Japan

<sup>c</sup> Data-driven Polymer Design Group, Research Center for Macromolecules and Biomaterials, National Institute for Materials Science, 1-2-1 Sengen, Tsukuba 305-0047, Japan

<sup>d</sup> Department of Physics, Faculty of Mathematics and Natural Sciences, Universitas Indonesia, Depok 16424, Indonesia

<sup>e</sup> Department of Mechanical & Industrial Engineering, University of Toronto, Toronto, Ontario M5S 3G8, Canada

<sup>f</sup> Faculty of Allied Health Sciences, Chettinad Hospital and Research Institute, Chettinad Academy of Research and Education, Kelambakkam 603103, Tamil Nadu, India

## ARTICLE INFO

## Keywords:

Saline soil  
Struvite  
Slow-release fertilizers  
Hydrogel beads encapsulated  
Sodium alginate  
Poly (acrylic acid)  
Humic acid

## ABSTRACT

Soil salinity, a severe environmental factor, significantly reduces the productivity of crop plants by increasing salt and mineral fertilizer concentrations in the soil. As a result, the development of sustainable slow-release mineral fertilizers (SRFs) is critical for addressing salt-affected soils. This study aimed to synthesize struvite ( $\text{MgNH}_4\text{PO}_4 \cdot 6\text{H}_2\text{O}$ ) into hydrogel beads made from sodium alginate-poly (acrylic acid) in the absence (Sa@S) and presence (Sa@SHa) of humic acid (HA). The optimal conditions for struvite formation were at pH 9.0, resulting in a remarkable 73.21 %, 98.74 %, and 99.20 % for Mg,  $\text{NH}_4\text{-N}$  and P removal, respectively. The SRFs study demonstrated that struvite had a significant release of Mg, P, and  $\text{NH}_4\text{-N}$ , notably higher ( $P \leq 0.05$ ) than Sa@S and Sa@SHa. Experiments on swelling and soil water loss demonstrated that Sa@S yielded higher results in comparison to Sa@SHa. Furthermore, an experiment was conducted to study the impact of Sa@S and Sa@SHa on saline soil parameters over 20 days of incubation. The results showed both encapsulated struvite hydrogel beads reduced soil salinity, as indicated by the sodium adsorption ratio (SAR) and exchangeable sodium percentage (ESP). Additionally, a significant reduction ( $P \leq 0.05$ ) in soil electrical conductivity (EC) and sodium (Na) was observed for both hydrogel bead encapsulation treatments compared to the control soil. However, no apparent variance was observed in pH and soil organic carbon (SOC). Moreover, the levels of available phosphorus (P), ammonium-nitrogen ( $\text{NH}_4\text{-N}$ ), nitrate-nitrogen ( $\text{NO}_3\text{-N}$ ), cation exchange capacity (CEC), and exchangeable cations (Ca, Mg, K) in the soil were observed to be increased ( $P \leq 0.05$ ).

## 1. Introduction

Soil salinization significantly threatens crop development and productivity, especially in arid and semiarid regions (Qadir et al., 2017). The overall extent of soil salinization affects approximately 1 billion hectares, accounting for about 7 % of the Earth's continental area, nearly ten times the size of Venezuela or twenty times France (Metter-lich and Zinck, 2003). Soil salinity represents a notable environmental

stress caused by excessive salt concentrations or significant amounts of exchangeable sodium ions (Na) in soil contents (Shahid et al., 2018). The build-up of salts in soils results in the degradation of soil properties, leading to a decline in osmotic potential, which can restrict water availability to root cells, consequently hampering plant growth (Ahmed et al., 2020; Ashraf and Harris, 2004). Cevheri et al. (2022) and Leogrande and Vitti (2019) have illustrated the adverse effects of soil salinity on plant development, primarily ascribed to its detrimental

\* Corresponding author at: Graduate School of Comprehensive Scientific Research, Program in Biological System Sciences, Prefectural University of Hiroshima, Shobara 727-0023, Japan.

E-mail address: [ho-harada@pu-hiroshima.ac.jp](mailto:ho-harada@pu-hiroshima.ac.jp) (H. Harada).

<https://doi.org/10.1016/j.arabjc.2024.105877>

Received 23 March 2024; Accepted 13 June 2024

Available online 14 June 2024

1878-5352/© 2024 The Authors. Published by Elsevier B.V. on behalf of King Saud University. This is an open access article under the CC BY-NC-ND license (<http://creativecommons.org/licenses/by-nc-nd/4.0/>).

impact on organic matter and nutrient cycling.

The solubility of chemical fertilizers is intimately tied to nutrient cycling processes and organic matter in the soil. Nutrient cycling involves the uptake of nutrients by plants, their release into the soil upon the breakdown of organic matter, and their subsequent availability for plant use (Grzyb et al., 2020). Organic matter is vital as it stores nutrients, supports microbial activity, and makes nutrients, including those in chemical fertilizers, more soluble and accessible to plants (Jamir et al., 2019; Rashid et al., 2016). High levels of organic matter enhance the soil's capacity to retain water and nutrients, facilitating the gradual release of nutrients from organic sources and chemical fertilizers. This improves overall nutrient availability to plants while reducing the risk of nutrient leaching (Malcolm et al., 2019). Additionally, organic matter contributes to soil aggregate stabilization, further impacting nutrient solubility and availability by influencing soil structure and porosity.

Conversely, nutrient cycling may not be as efficient in soil with low organic matter content, necessitating a greater reliance on soluble chemical fertilizers to meet plants' essential nutrient requirements. However, the effectiveness and solubility of these chemical fertilizers can be influenced by various factors, including pH level, electrical conductivity (EC), and the content of sodium (Na), potassium (K), magnesium (Mg), and calcium (Ca) (Fageria et al., 2014; Moreira et al., 2015). Moreover, metrics such as sodium absorption ratio (SAR) and exchangeable sodium percentage (ESP) provide valuable insights into establishing optimal chemical conditions within the soil component (Shirokova et al., 2000). Evaluating soil salinity and sodicity typically involves measuring EC, SAR, and ESP parameters. Soils containing lower values of EC (<4 mS/cm), SAR (<13), and ESP (<15 %) are generally considered natural and non-sodic soil (Shrivastava and Kumar, 2015; Tanehgonbadi and Qaderi, 2023). EC values indicate soil salinity levels, while SAR and ESP values reflect the amount of Na in the soil.

Several management strategies have been successfully employed to alleviate the adverse effects of salt-affected soils. For instance, Zahedifar (2020) demonstrated that biochar made from sugarcane bagasse could immobilize cadmium (Cd) under saline soil conditions. Another study by Zhang et al. (2020) reported that incorporating gypsum and biochar into salty soils improved their water properties. Liang et al. (2021) also discovered that biochar can improve porosity, field capacity, and plant-accessible water in saline-alkali soils. Abdel-Fattah (2012) has reported the significant impact of composts and gypsum on the restoration of saline-sodic soils and soil pH, EC, ESP, and SAR. But then, Elrashidi et al. (2010) discovered that gypsum decreases the solubility of phosphorus (P), iron (Fe), zinc (Zn), copper (Cu), and boron (B) in soils, limiting their accessibility to plants. Moreover, high concentrations of minerals such as Mg, Na, K, and Ca in the soil can also contribute to its salinity (Kumar and Sharma, 2020; Munns et al., 2020; Zhao et al., 2020). Therefore, there is a need for innovative approaches to delay nutrient release in the soil and minimize its impact on plants and the environment.

Slow-release fertilizers (SRFs) have recently shown significant promise in enhancing fertilizer usage efficiency, delaying the nutrient release or increasing the availability of nutrients over time, and mitigating the environmental issues associated with fertilizer management (Qiao et al., 2016). Struvite, a well-recognized product derived from P recovery, is classified as SRFs because of its limited solubility and varied nutrient composition (Rech et al., 2018). SRFs are specifically formulated to deliver nutrients slowly and steadily to plants, match their nutritional needs, and minimize nutrient loss. Although struvite is typically used as a P fertilizer, it also comprises considerable levels of Mg and N. According to Wang et al. (2023), struvite can reduce N loss by up to 58.1 % and decrease nitrous oxide (N<sub>2</sub>O) emissions, unlike traditional N fertilizers, which contribute to global warming (Liang et al., 2007).

Recently, hydrogel presented a promising alternative to conventional saline soil management methods (Tefera et al., 2022). It absorbs water and gradually releases it to the surrounding soil (Li and Zhang, 2023). This carefully regulated water release improves water utilization

and reduces salt build-up. Sodium alginate (Na-Alg) is a bio-based hydrogel with hydrophilic characteristics and a harmless polymer with a high swelling capacity (Satheesh Kumar et al., 2023). This property makes it capable of reducing the contact of Na<sup>+</sup> and Cl<sup>-</sup> ions in the soil through cation exchange capacity (Niu et al., 2020). However, Na-Alg may not distribute uniformly throughout the soil profile when applied to the soil, leading to uneven water and nutrient absorption and localized high salt concentrations around the hydrogel particles. In contrast, hydrogel beads may offer better control over soil distribution, helping minimize localized salt concentrations. The stability of Na-Alg hydrogel beads is limited in an excessive ionic interaction or the presence of specific ions. The use of poly (acrylic acid) (Poly-Acr) can enhance the stability and mechanical strength of hydrogel composite (Faturechi et al., 2015). Humic acid (HA) is widely recognized for its beneficial role in improving soil properties and enhancing the utilization rate of fertilizers. It contains a significant concentration of organic carbon, which enhances the activities of antioxidant enzymes and alleviates the effects of salinity stress in soil (Chen et al., 2017). Studies have demonstrated that HA can enhance soil fertility, improve plant development (Li et al., 2019) and improve soil's water-holding capacity (Ennab et al., 2023). Additionally, it can improve the stability of hydrogels (Venezia et al., 2022).

The use of encapsulation techniques to contain chemicals such as fertilizers (Abd El-Aziz et al., 2022; Olad et al., 2018; Qiao et al., 2016), pesticides (de Oliveira et al., 2020), and herbicides (Nörnberg et al., 2019) has been reported to reduce their volatility and minimize toxicity, as well as improve environmental control (Atalay et al., 2022). Accordingly, we hypothesize that the encapsulation of struvite within hydrogel beads can control nutrient release, reduce salt toxicity, and enhance soil properties. In this study, we employed various pH conditions to synthesize struvite using solutions containing Mg, NH<sub>4</sub>-N, and P. Following this, the struvite was coated with hydrogel beads created from a combination of Na-Alg and Poly-Acr, with and without the addition of HA. To analyze the struvite, X-ray diffraction (XRD) was utilized, while scanning electron microscopy (SEM), energy dispersive X-ray spectroscopy (EDS), and Fourier transform infrared spectroscopy (FTIR) were used to analyze the hydrogel beads. This study investigated a promising sustainable approach to managing mineral fertilizers' discharge and identified environmentally acceptable alternatives to enhance and mitigate soil quality in saline areas.

## 2. Materials and method

### 2.1. Materials

Calcium chloride (CaCl<sub>2</sub>, 99 %), hydrochloric acid (HCl, 36.5–38 %), sodium carbonate (Na<sub>2</sub>CO<sub>3</sub>, >99.8 %), sodium dihydrogen phosphate (NaH<sub>2</sub>PO<sub>4</sub>, >99.95 %), ammonium acetate (CH<sub>3</sub>COONH<sub>4</sub>, >97 %), and sodium hydroxide (NaOH, 99.99 %) were procured from Kanto Chemical Co. Inc., Japan. Humic acid and sodium alginate were purchased from Wako Chemicals, Tokyo, Japan. The poly (acrylic acid) (molecular weight: 100,000) was obtained from Scientific Polymer Products, INC., New York. All the reagents were of analytical grade, and deionized water was used throughout the experiments.

### 2.2. Preparation of struvite precipitation

Deionized water (DI) was used to prepare stock solutions of MgCl<sub>2</sub>, NH<sub>4</sub>Cl, and NaH<sub>2</sub>PO<sub>4</sub> at room temperature. These solutions were mixed in a ratio of 1:1:1, with equal concentrations of Mg, NH<sub>4</sub>-N, and P. The pH of the solution was adjusted to 8.0, 8.5, 9.0, 9.5, and 10.0 by gradually adding 0.1 M NaOH solution under magnetic stirring for 15 min. The solution was allowed to age overnight to ensure uniformity and was filtered to determine the Mg, NH<sub>4</sub>-N, and P removal percentage (Removal, (%)) using Eq. (1) (Hidayat et al., 2023). The resulting solid residue was dried in an oven at 60 °C for 48 h for further analysis.

$$\text{Removal, (\%)} = \frac{C_i - C_e}{C_i} \times 100 \quad (1)$$

where Removal, (%) is the removal efficiency, and  $C_i$  and  $C_e$  are the initial and equilibrium phosphorus concentrations (mg/L), respectively.

### 2.3. The procedure to encapsulate struvite in hydrogel bead

This study utilized struvite obtained from a pH of 9.0 as the additional material to produce hydrogel beads encapsulation. Encapsulating struvite within hydrogel beads was carried out at room temperature. To prepare Sa@S, a combination of 6 mL of 2 wt% Na-Alg aqueous solution, 6 mL of 5 wt% Poly-Acr aqueous solution, 1 mL of 3 M NaOH, and 0.1 g of struvite was mixed and agitated in bottle flasks for 1 h. The mixture was then slowly injected into a 10 wt%  $\text{CaCl}_2$  aqueous solution using a 10 mL syringe. The resulting hydrogel beads were left to grow overnight to facilitate crosslinking. Afterward, the hydrogel beads were washed with ethanol, DI, and dried in an oven at 25 °C for 24 h. The method for encapsulating Sa@SHa hydrogel beads involved substituting 3 M NaOH with HA solution. To prepare HA, a mixture of 3 M NaOH (20 mL) and 0.1 g of HA was allowed to react at room temperature for 24 h, after which the solution was filtered through filter paper.

### 2.4. Characterization of hydrogel beads

The crystalline structure of struvite was examined using powder X-ray diffraction (XRD) with Cr/ $K\alpha$  radiation ( $\lambda = 2.2909 \text{ \AA}$ , MiniFlex, Rigaku, Japan). The functional groups of struvite and hydrogel bead encapsulation were evaluated using a Nicolet iS10 FTIR analyzer (Thermo Fisher Scientific Inc., Waltham, MA, USA). The morphology structure image and chemical composition of struvite and hydrogel beads were analyzed using a benchtop scanning electron microscope (SEM) linked with energy dispersive X-ray spectroscopy (EDS) Miniscope TM-4000PlusII (Hitachi-Hitech, Tokyo, Japan).

### 2.5. Determination of mineral release

The quantities of Mg, Ca, P, and  $\text{NH}_4\text{-N}$  released from the hydrogel beads were assessed via batch water shaker experiments (BW101, Yamato, Japan). Each set of beads (0.5 g) was placed in 50 mL of DI and agitated at 25 °C with a speed of 100 rpm. Nutrient analysis (Mg, Ca, P, and  $\text{NH}_4\text{-N}$ ) was performed at intervals of 3 hours, 3 days, 7 days, and 14 days.

### 2.6. Swelling experiments analysis

The swelling characteristics of the hydrogel bead-encapsulated was assessed. In brief, dried hydrogel beads were immersed in a glass beaker containing 50 mL of DI. The experiments were conducted using water batch shaker (BW101, Yamato, Japan) at 25 °C for 24 h and the swelling rate was calculated using the following Eq. (2) (Hidayat et al., 2024a).

$$\text{Swelling rate (\%)} = \frac{W_s - W_d}{W_d} \times 100 \quad (2)$$

where  $W_s$  is the weights of swollen hydrogels and  $W_d$  is the weights of dried hydrogels.

### 2.7. Soil incubation experimental design

Soil was obtained from a store in Shobara City, with a pH value of  $5.60 \pm 0.85$ , electrical conductivity (EC) of  $119 \mu\text{S}/\text{cm} \pm 26.87$ , cation exchange capacity (CEC) of  $1.09 \text{ me}/100 \text{ g} \pm 0.78$ , available phosphorus (P) content of  $2.71 \text{ mg}/\text{kg} \pm 0.60$ , and a C/N ratio of  $15.59 \pm 0.17$ . This soil was utilized in the preparation of artificial salt-soil. A mixture of 1 kg of air-dried soil samples and 2 L of a 250 mM NaCl

solution was prepared in a plastic container. The soil and solution were then incubated together for three days. Afterward, the soil was filtered and dried in an oven at 60 °C for three days. A soil salinity experiment was conducted over 20 days using an experimental design that included three conditions: a control group with only soil, a group with soil treated with 2 wt% Sa@S, and a group with soil treated with 2 wt% Sa@SHa. The temperature of the experimental environment was maintained at a constant 25 °C. Hydrogel bead samples were placed in plastic cups and soaked with deionized water to reach 25 % of the soil's water-holding capacity. Around 30 g of soil samples were collected from each cup at intervals of 5, 10, and 20 days and dried in an oven at 60 °C for three days for further analysis.

### 2.8. Soil water loss analysis

We measured soil water loss rate (SWL rate) in the saline soil over a period of 7 days. 100 g of dried saline soil is placed into plastic container and subsequently, the dried hydrogel beads were added. The saline soil was then watered with DI and weighed ( $W_i$ ). The containers were kept in the laboratory under ambient air and temperature conditions and were weighed from 1, 2, 4 and 7 days ( $W_t$ ). The SWL rate was calculated using Eq. (3) (Rabat et al., 2016).

$$\text{SWL rate (\%)} = \frac{W_i - W_t}{\text{Soil Weight (g)}} \times 100 \quad (3)$$

### 2.9. Determination of soil compositions

The pH and EC was measured by mixture of soil and DI water at proportion of 1:5 (w/v) was agitated for 30 min. To measure the amount of available phosphorus, a 0.5 M  $\text{NaHCO}_3$  solution was used at a 1:20 (w/v) ratio for 30 min according to the Olsen technique (Hidayat et al., 2024b). The molybdenum method blue method was employed to determine the phosphorus content by measuring at the wavelength of 693 nm. For determining the amount of exchangeable cations (Ca, K, Mg, and Na), 1 N  $\text{CH}_3\text{COONH}_4$  extraction method was utilized, followed by adding 10 wt% NaCl to determine the soil's CEC. The available  $\text{NH}_4\text{-N}$  and  $\text{NO}_3\text{-N}$  content in the soil was obtained using 2 M KCl at a ratio of 1:10 (w:v) for 2 h. The determination of soil organic carbon (SOC) can be quantified using Walkley and Black's wet oxidation method (Hidayat et al., 2024b).

### 2.10. Analysis of sodium adsorption ratio and exchangeable sodium percentage

The interaction between the sodium adsorption ratio (SAR) and exchangeable sodium percentage (ESP) and the concentration of Mg, Ca, and K in the water extract derived from saturated soil can be represented mathematically using Eqs. (4) and (5) (Tefera et al., 2022).

$$\text{SAR} = \frac{\text{Na}}{\sqrt{\frac{1}{2}(\text{Mg} + \text{Ca})}} \quad (4)$$

$$\text{ESP} = \frac{\text{Na}}{\text{Na} + \text{K} + \text{Ca} + \text{Mg}} \times 100 \quad (5)$$

### 2.11. Statistical analysis

Data analysis was carried out using MINITAB software, specifically version 21.3.1. Statistical analysis was conducted using one-way analysis of variance to examine mean values, and Tukey's test was used to compare treatments ( $P \leq 0.05$ ).

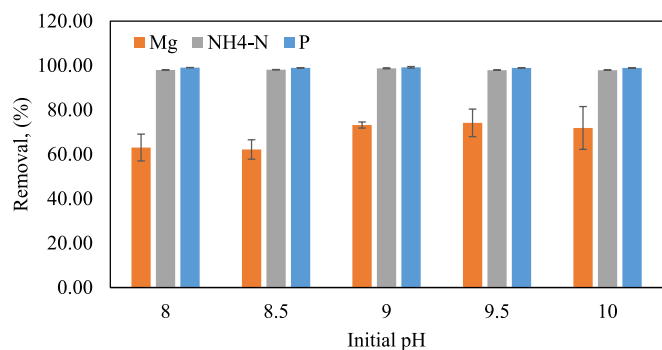


Fig. 1. Initial pH precipitation solution versus removal percentage.

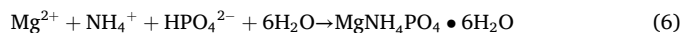
### 3. Results and discussion

#### 3.1. Characterization of precipitation

The experiment was conducted by mixing equal volumes and concentrations of Mg, NH<sub>4</sub>-N, and P solutions at various pH levels ranging from 8 to 10. The results showed that the highest Mg, NH<sub>4</sub>-N and P removal percentage at pH 9.0 with value of 73.21 %, 98.74 %, and 99.20 %, respectively. However, as the pH increased to 10.0, the removal percentage decreased (Fig. 1). This suggests that there may have been additional compounds that precipitated alongside the struvite. These results are consistent with the study conducted by (Zhou and Chen, 2019) which used electrochemical techniques to produce struvite precipitates. Fig. 2 shows SEM micrographs of the residues obtained from different pH conditions. Regardless of pH, each crystal possessed a needle-shaped structure. Moreover, pH has a particular influence on the size of the crystal. Due to increased nucleation density, crystals will typically be smaller at higher pH. The largest crystal size was recorded at

pH 8.0, while the smallest size was observed at pH 8.5. In addition, Fig. 2a–e presents the SEM images and assemblies of the C, O, N, P, and Mg maps, respectively. Notably, the samples contain significant amounts of N, P, K grains, which are prominent characteristics. Although the elemental maps of C, O, N, P, and Mg appear similar, the grains exhibit varying signal intensities (Table 1).

The XRD spectrum of the precipitate shown in Fig. 3 matched that of the struvite registered in the Powder Diffraction File (PDF) database (JCPDS 00–015–0762). The EDS data were used to examine the composition of the precipitation surface. The findings in Table 1 indicate that at pH 9.0, the maximum atom percentages of N, P, and Mg were obtained. This discovery corresponds to the formation of struvite precipitates (as seen in Eq. (6)) and is consistent with the study reported by (González-Morales et al., 2021).



#### 3.2. Characteristics of encapsulation

The structure of the struvite encapsulated within hydrogel beads was analyzed using scanning electron microscopy (SEM). Fig. 4 and Fig. 5 corresponds to Sa@S and Sa@SHa, respectively. The hydrogel beads

Table 1

EDS data composition of struvite precipitation in different pH conditions.

pH	Composition (Atom %)				
	C	O	N	P	Mg
8.0	61.75	31.42	3.82	1.27	1.74
8.5	56.90	35.00	3.97	1.84	2.29
9.0	39.28	47.41	3.86	5.01	4.43
9.5	51.45	38.81	3.89	2.40	3.45
10.0	54.94	36.65	3.40	2.09	2.92

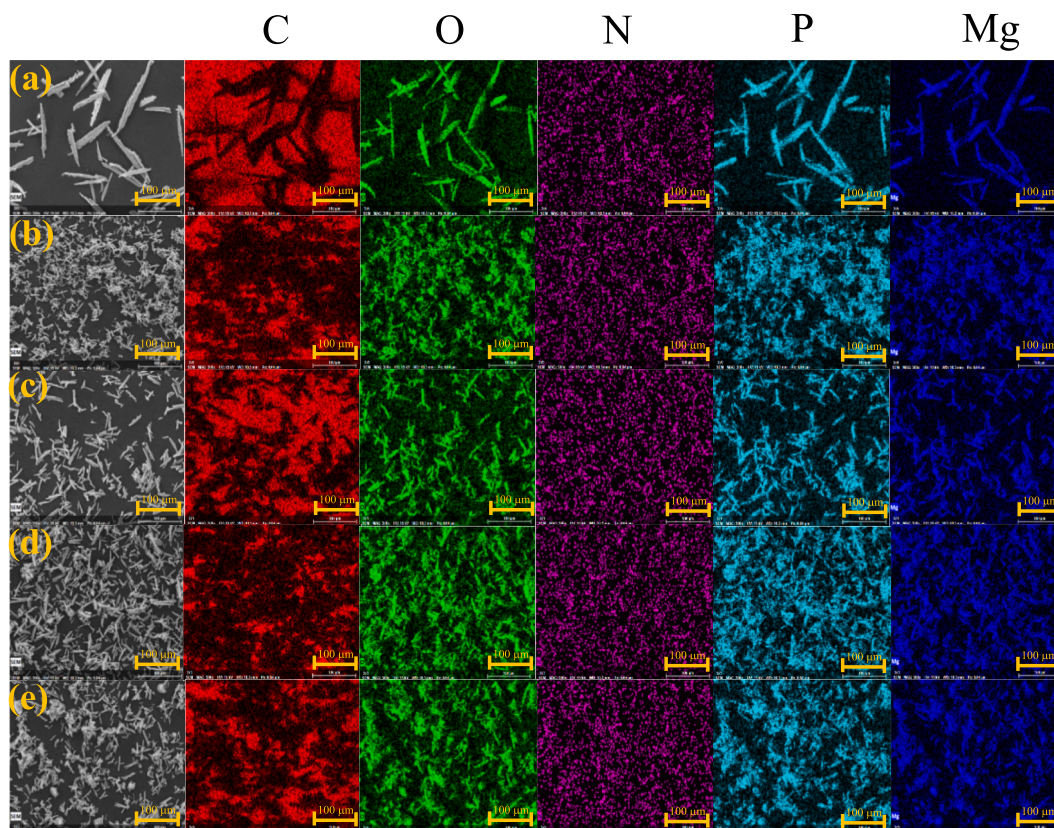


Fig. 2. SEM images and EDS mapping of solid residue in different pH conditions (a) pH 8 (b) pH 8.5 (c) pH 9 (d) pH 9.5 (d) pH 10.

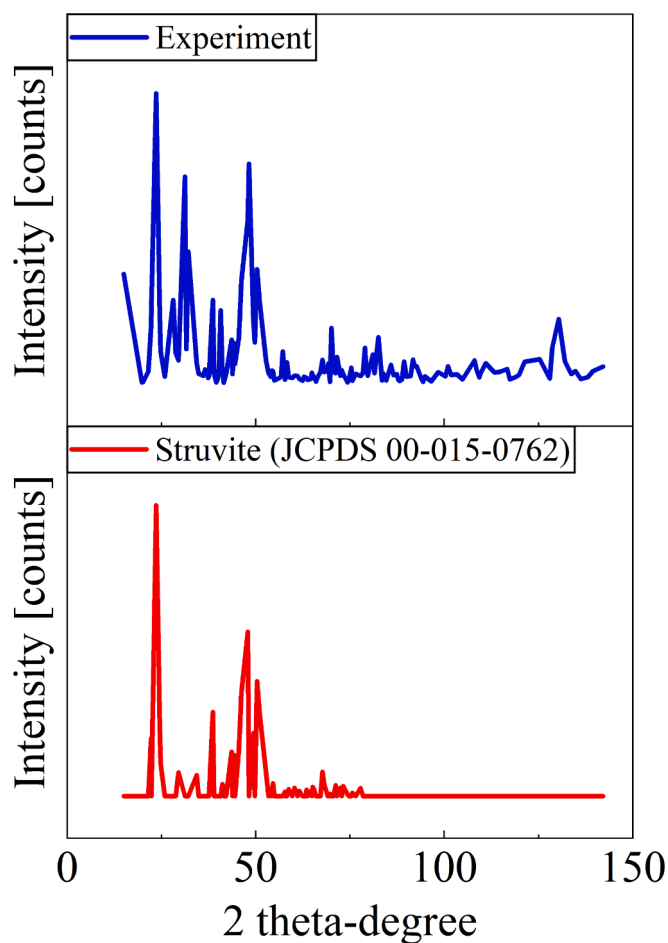


Fig. 3. XRD spectra of struvite collected at pH 9.0 condition and struvite (JCPDS 00–015–0762).

were microscopically tiny, exhibiting a sponge-like structure with interconnected pores (Fig. 4a and Fig. 5a). The size of the pores gradually increased from the surface to the interior of the Sa@S hydrogel beads (Fig. 4b). The addition of HA was found to enhance the formation of hydrogel networks. The introduction of HA resulted in a change in the structure of the hydrogel beads, producing a smooth surface (Fig. 5a). Fig. 5c illustrates the fibrous morphology of the hydrogel beads, which have interconnected pores on both the inside and outside of the beads. Upon closer examination, struvite crystals were observed on the surfaces of both the Sa@S (Fig. 4f) and Sa@SHa (Fig. 5f) hydrogel beads encapsulation. The fabrication process successfully encapsulated the struvite within the hydrogel beads, effectively regulating the release of minerals from the beads.

FTIR spectroscopy was utilized to investigate the functional groups within a molecule. The FTIR results for struvite, Sa@S, and Sa@SHa are depicted in Fig. 6a. Peaks detected between  $3227\text{ cm}^{-1}$  and  $3346\text{ cm}^{-1}$  were attributed to the elongation of O–H bonds, as described by researchers (Das et al., 2023). Peaks identified between  $2896\text{ cm}^{-1}$  and  $2924\text{ cm}^{-1}$  indicated the stretching of N–H bonds (Valle et al., 2022). The bending frequency of water molecules was verified to be approximately  $1650\text{ cm}^{-1}$  (Valle et al., 2022). The peak at around  $1541\text{ cm}^{-1}$  suggested the presence of COO groups formed by the combination of sodium alginate and poly (acrylic acid) (Hua et al., 2010). The wavenumbers  $1328\text{ cm}^{-1}$  and  $1028\text{ cm}^{-1}$  corresponded to the bending vibrations of O–H bonds and C–O–C bond stretching, respectively (Hua et al., 2010). The peak at  $971\text{ cm}^{-1}$  corresponded to the symmetric stretching of the phosphate group, while a peak at  $754\text{ cm}^{-1}$  was correlated to the elongation of P–O–P bonds (Bogdan et al., 2021). The

peak at  $884\text{ cm}^{-1}$  may have been responsible for cubic MgO (Chinthakuntla et al., 2016; Ding et al., 2001). Research conducted by (Chinthakuntla et al., 2016) revealed that the stretching vibration of Mg–O occurred within the spectral region  $550\text{--}670\text{ cm}^{-1}$ .

### 3.3. Mineralization release rate, swelling and soil water loss study

This present study investigated the mineral release profiles of struvite, Sa@S, and Sa@SHa hydrogel bead composites using distilled water at a controlled temperature of  $25\text{ }^{\circ}\text{C}$  for duration ranging from 3 hours to 14 days. The findings demonstrate that struvite exhibits a greater ease of dissolution, leading to a significantly higher release of all nutrients, including Mg,  $\text{NH}_4\text{-N}$ , and P, compared to the encapsulated formulations of Sa@S and Sa@SHa, as shown in Fig. 6b. The average release rates of struvite were  $47.11\text{ mg/L}$ ,  $10.96\text{ mg/L}$ , and  $16.95\text{ mg/L}$  for Mg,  $\text{NH}_4\text{-N}$ , and P, respectively, whereas for Sa@S, they were  $7.81\text{ mg/L}$ ,  $0.49\text{ mg/L}$ , and  $1.64\text{ mg/L}$ . This indicates a difference of approximately 83.43 %, 90.35 %, and 95.54 % in nutrient release. Similarly, for Sa@SHa, the average release rates were  $7.81\text{ mg/L}$ ,  $0.49\text{ mg/L}$ , and  $1.64\text{ mg/L}$  for Mg,  $\text{NH}_4\text{-N}$ , and P with percentage difference of 88.14 %, 98.56 %, and 93.55 %. These percentage differences may be attributed to the barrier effect of the polymer hydrogels, hindering nutrient release. Furthermore, Sa@SHa showed higher percentage difference for struvite compared to Sa@S. This is due to the complex and intricate structure formed by the layers of HA, which obstructs the movement of minerals through the polymer network and into the surrounding environment.

Additionally, the concentration of Ca showed a higher rate of release during the initial 3-hours period but then decreased significantly over 14 days for both hydrogel bead encapsulations (Fig. 6c). This decline may be due to the higher concentration of Ca observed on the surface of the hydrogel beads, which act as cross-linkers and allow for the faster dissociation of Ca from the hydrogel beads.

The process by which minerals are released from hydrogel beads can be described as follows: the struvite utilized in the formulations is in the form of hydrogel beads. Upon adding the sample into water, the hydrogel undergoes water absorption and swelling, resulting in the dissolution of the mineral. The dissolved mineral is gradually released into the water through the polymeric shell due to the kinetic movement of water in the hydrogel and release medium. The difference in the concentration of soluble material between the internal and external conditions of the hydrogel bead primarily determines the rate of mineral release. However, the release rate slows down as the difference decreases over time.

Fig. 6d illustrates the swelling percentage of the hydrogel beads encapsulation. The data regarding swelling percentage indicate that Sa@S exhibits a higher rate of swelling than Sa@SHa. This is most likely due to the crosslinks formed by HA, which can constrain the movement of polymer chains and diminish the overall flexibility of the hydrogel network. Consequently, the hydrogel beads may reduce capacity to swell in response to water absorption. Fig. 6e presents the percentage of SWL rate for up to 7 days. The findings suggest that Sa@S hydrogel beads demonstrate significant water retention capability, with the lowest SWL rate recorded at 47 %. Conversely, Sa@SHa exhibits a value of 52 %. This showed that inclusion of HA into hydrogel beads has an unfavourable effect on swelling and soil water loss. In contrast, the SWL rate of intact saline soil was observed to be 78 %. It can be concluded that the introduction of hydrogel beads into the soil has a positive effect on water retention in the soil, as indicated by a reduction in soil water loss.

### 3.4. Assessment of soil quality

#### 3.4.1. Soil pH, EC, SAR, and ESP

Soil pH is vital in detecting soil quality because low and high pH levels can affect nutrient availability, soil structure, and microbial activity, impacting the plant growth (Zhang et al., 2019). The saline soil

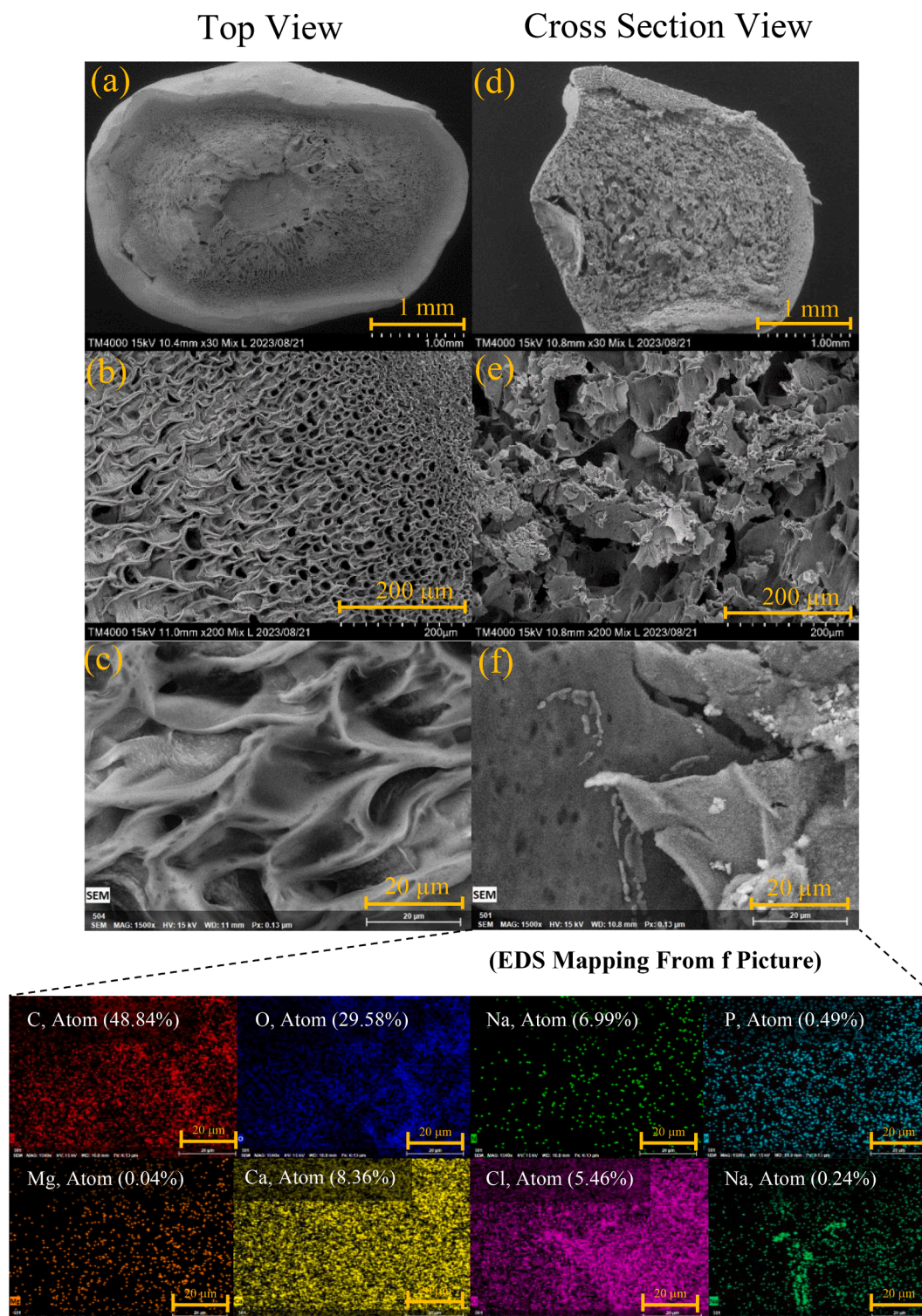


Fig. 4. SEM picture and EDS mapping of Sa@S hydrogel bead.

incubation experiment was conducted for 20 days. The results showed that the soil pH remained stable and unaffected by the treatment and incubation conditions ( $p \leq 0.05$ ) (Fig. 7a).

Similarly, high EC levels can hinder plant water uptake and lead to osmotic stress (Ding et al., 2018). The results show that there was a significant interaction between the treatments on EC ( $p \leq 0.05$ ) (Fig. 7b), which showed a substantial decline over the incubation period. After 5 days of incubation, using Sa@SHA in saline soil reduced EC from 6.09 mS/cm in the control treatment to 4.88 mS/cm and 5.41

mS/cm for Sa@S, respectively. After the incubation period (20 days), the control treatment (soil) was 6.61 mS/cm, while Sa@S and Sa@SHA treatment reached 3.83 and 3.52 mS/cm, respectively. These values indicate that the soil is normal (Negacz et al., 2022), and suggest that the encapsulation of hydrogel beads served as a barrier, effectively inhibiting excessive nutrient leaching and promoting water retention, resulting in decreased soil electrical conductivity.

The SAR and ESP are essential indicators of soil salinity and sodicity, respectively, significantly impacting crop growth (Andrade Foronda and

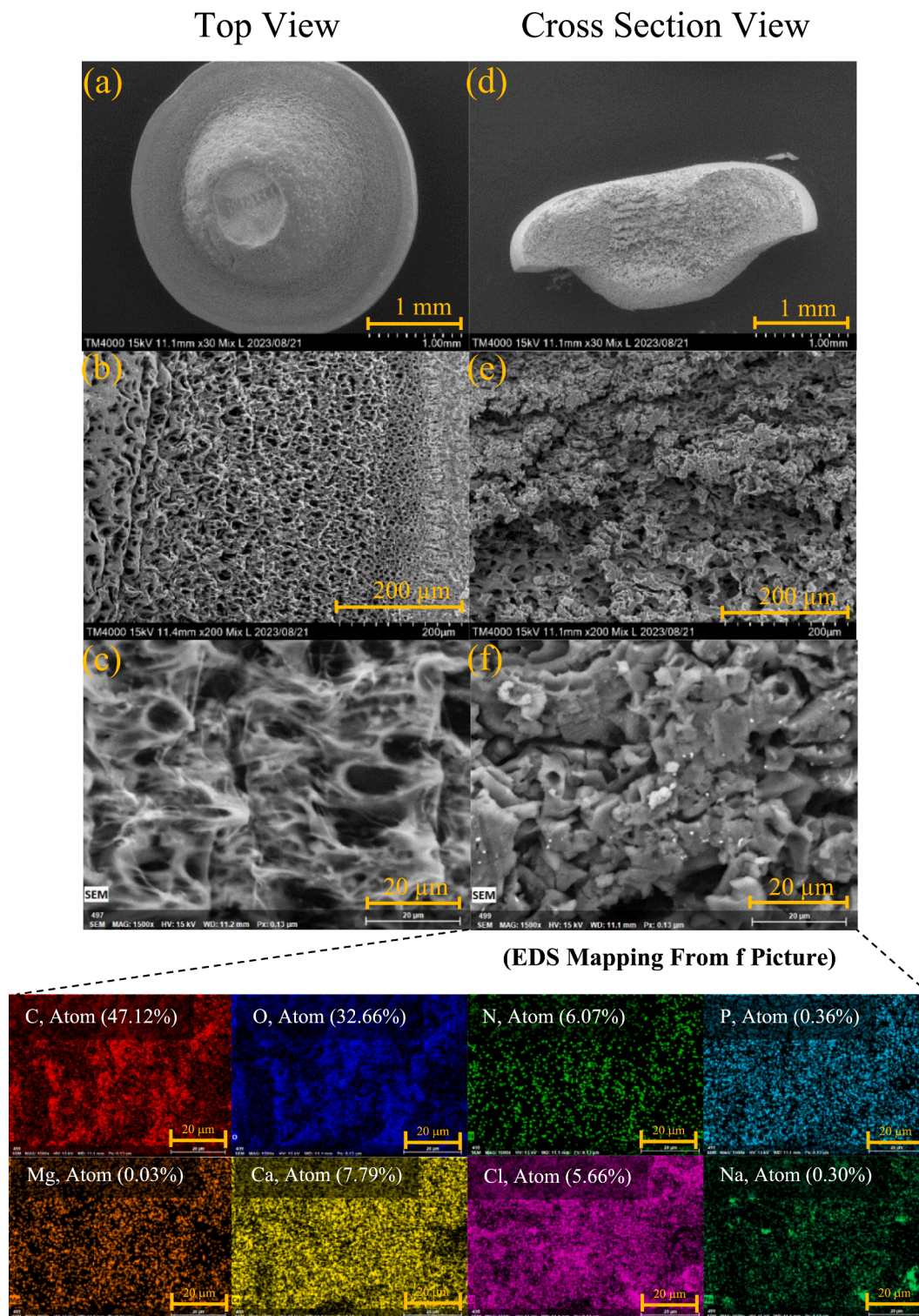
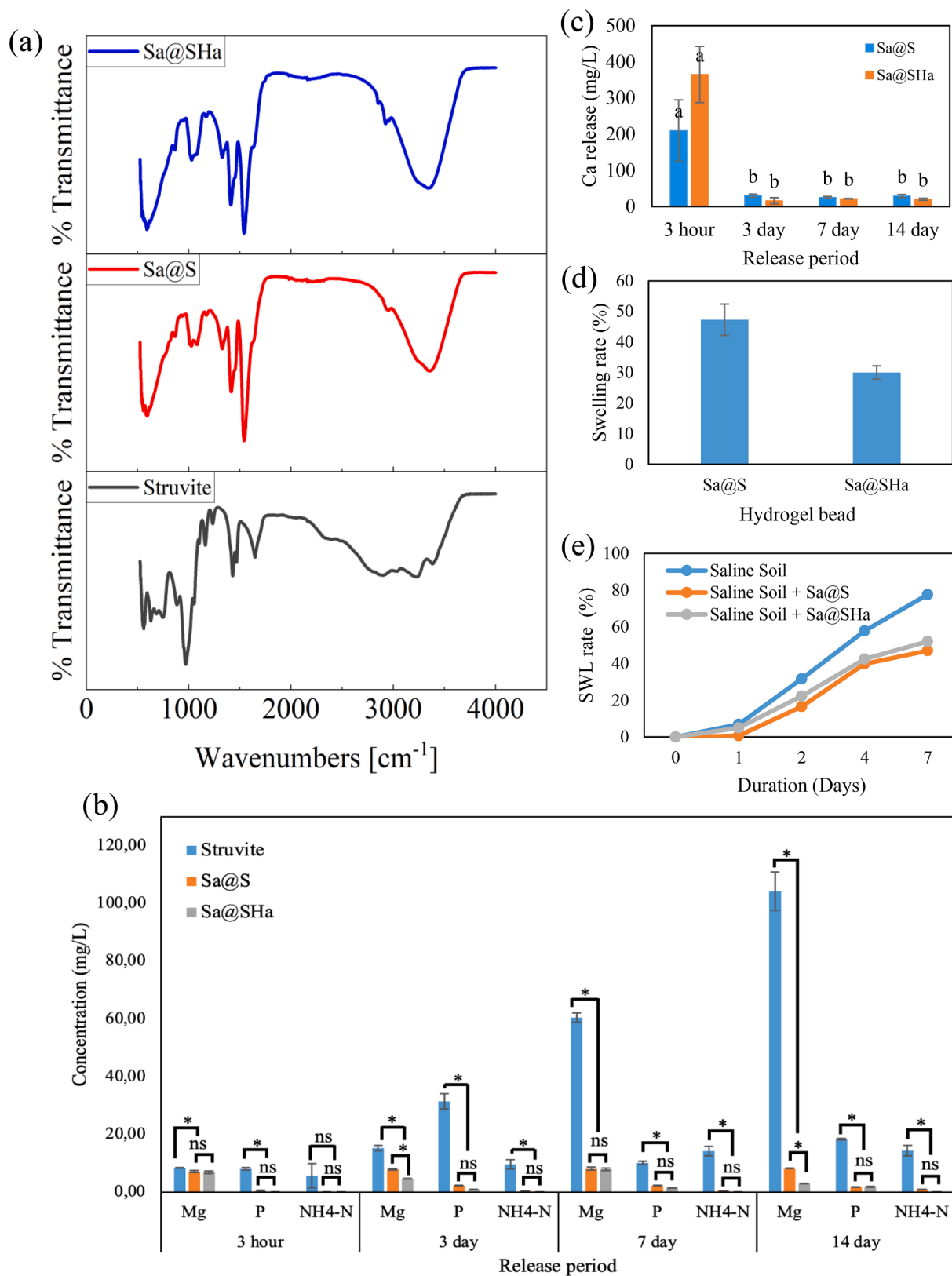


Fig. 5. SEM picture and EDS mapping of Sa@SHa hydrogel bead.

Colinet, 2023; Gharaibeh et al., 2021). SAR measures the ratio of Na ions to Ca and Mg ions in the soil solution, and elevated SAR values indicate higher Na levels that can harm soil structure, reduce water infiltration, impede nutrient retention, and restrict root development. As shown in Table 2, all treatments exhibited varying SAR values. The application of hydrogel bead encapsulation, particularly the use of Sa@SHa, resulted in the most significant reduction in SAR levels, with a decrease of 60.58 % from 27.73 to 10.93, followed by Sa@S with a reduction of 54.09 % compared to the soil only.

The ESP represents the proportion of exchangeable sodium concerning the total exchangeable cations (including Na, Mg, Ca and K) in the soil. High ESP values suggest a greater Na concentration than other cations, leading to soil dispersion and reduced permeability. This can negatively impact root penetration and nutrient absorption in crops. The ESP values after incubation are presented in Table 2, which indicates that all treatments had ESP values below 12 following the incubation period. However, after 20 days of incubation, the application of hydrogel bead encapsulation resulted in the lowest values, measuring



**Fig. 6.** (a) FTIR spectra of struvite pH 9.0, Sa@S, and Sa@SHa (b) Comparison nutrient release from struvite pH 9.0, Sa@S, and Sa@SHa (c) Ca release from hydrogel beads (Sa@S and Sa@SHa) (d) Swelling rate of Sa@S and Sa@SHa (e) Soil water loss of Sa@S and Sa@SHa under salinity. \*Indicates statistically significant at a significance level of  $P \leq 0.05$ ; ns denotes no significant difference in Tukey's test.

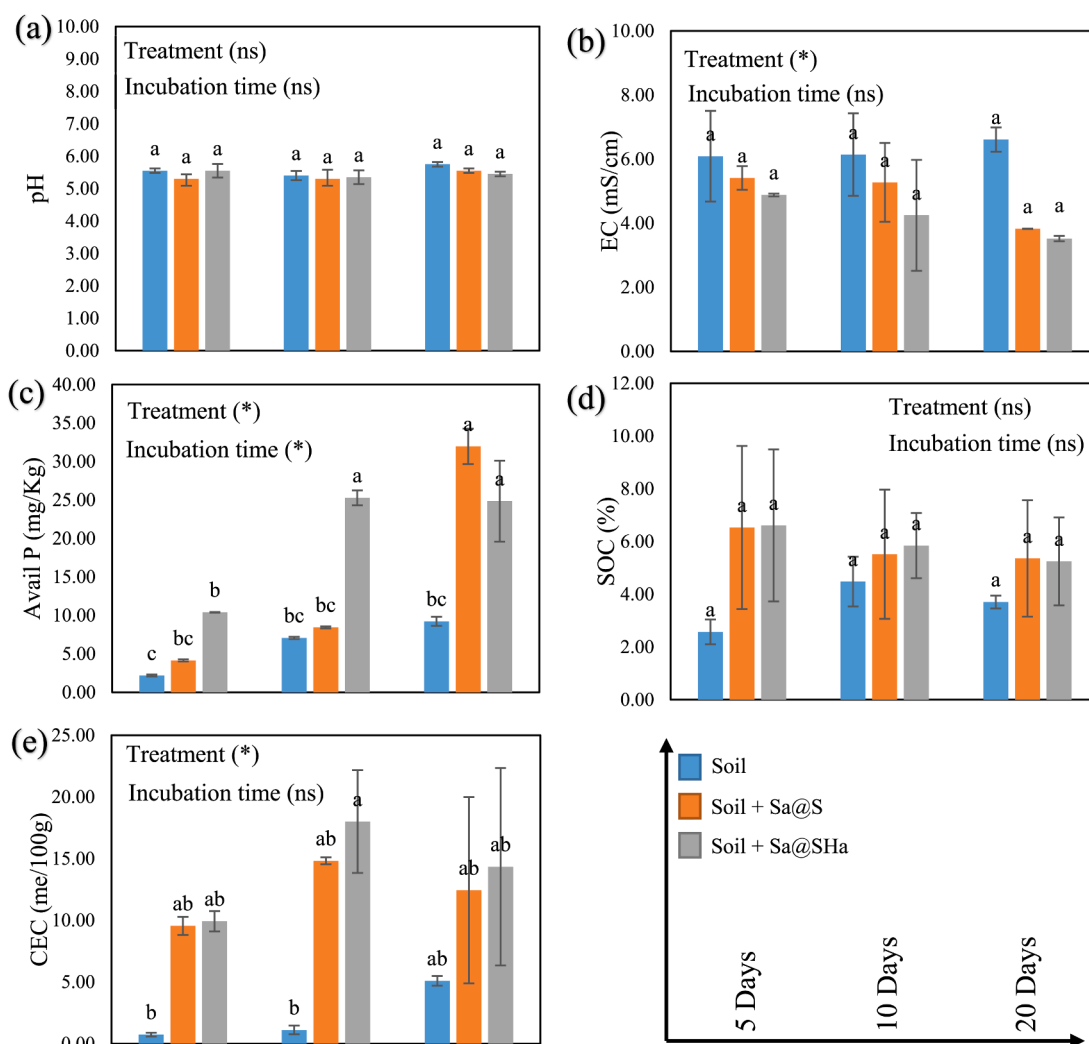


**Fig. 7.** Soil characteristics (pH, EC, available P, SOC, and CEC) in saline soil regarding hydrogel beads application at different incubation times. The vertical bars indicate the mean standard error. Avail: Available. Control: soil only, Sa@S: soil + Sa@S samples, Sa@SHa: soil + Sa@SHa samples. Statistically significant at a significance level of  $P \leq 0.05$  in Tukey's test.

**Table 2**  
Effect of hydrogel bead on SAR and ESP value.

Treatment	SAR						ESP											
	Incubation time (days)						Incubation time (days)											
	5	10	20	5	10	20	5	10	20	5	10	20						
Soil (Control)	41.86	41.52	27.73	8.30	11.87	9.01	17.49	22.58	12.73	5.92	6.85	2.63	14.69	22.15	10.93	4.68	6.16	2.65
Soil + Sa@S																		
Soil + Sa@SHa																		

2.65 and 2.63 for Sa@S and Sa@SHa, respectively. These values classify the soil as non-sodic, as described by (Tanehgonbadi and Qaderi, 2023). These findings align with (Abdeen and Saeed, 2019), who used hydrogels derived from poly (vinyl alcohol) borate to remediate saline and sodic conditions and restore soil to its normal state.

### 3.4.2. Phosphorus and organic carbon

P is an indispensable nutrient for the development and growth of plants, performing a vital function in photosynthesis, energy transfer, and root formation. Adequate P levels in the soil are essential for optimal plant growth and productivity (Bechtaoui et al., 2021; Victor Roch et al., 2019). The results of the study demonstrated that the amount of

available P in the saline soil increased significantly over time in all treatments compared to the soil (control) treatment (Fig. 7c). Statistical analysis showed a remarkable relationship between treatment and incubation period ( $P \leq 0.05$ ). After five days of incubation, the soil treatment showed the lowest concentration of available P. However, the soil treated with Sa@S exhibited the most significant increase in available P content after incubation. The available P concentration in the study was primarily 2.18, 4.14, and 10.40 mg/Kg for soil, Sa@S, and Sa@SHa, respectively. After 20 days of incubation, the values for soil, Sa@S, and Sa@SHa increased to 9.23, 31.96, and 24.85 mg/Kg, respectively. In contrast, SOC value revealed there was no notable difference for all treatments and incubation periods ( $P \leq 0.05$ ) (Fig. 7d). This may be attributed to the presence of struvite-encapsulated hydrogel beads, which can exacerbate stress and further limit the activity of soil organisms involved in the decomposition of organic matter.

### 3.4.3. Cation exchange capacity and exchangeable cations

CEC refers to the capacity of soil to retain and exchange cations such as Ca, Mg, K, and Na. Higher CEC soil content can retain more nutrients, making them more fertile (Razzaghi et al., 2021). The difference in the soil CEC was significant ( $P \leq 0.05$ ) throughout all treatments, as shown in Fig. 7e. Overall, the application of both hydrogel beads showed a substantial increase in CEC ( $P \leq 0.05$ ) compared to soil (control) with

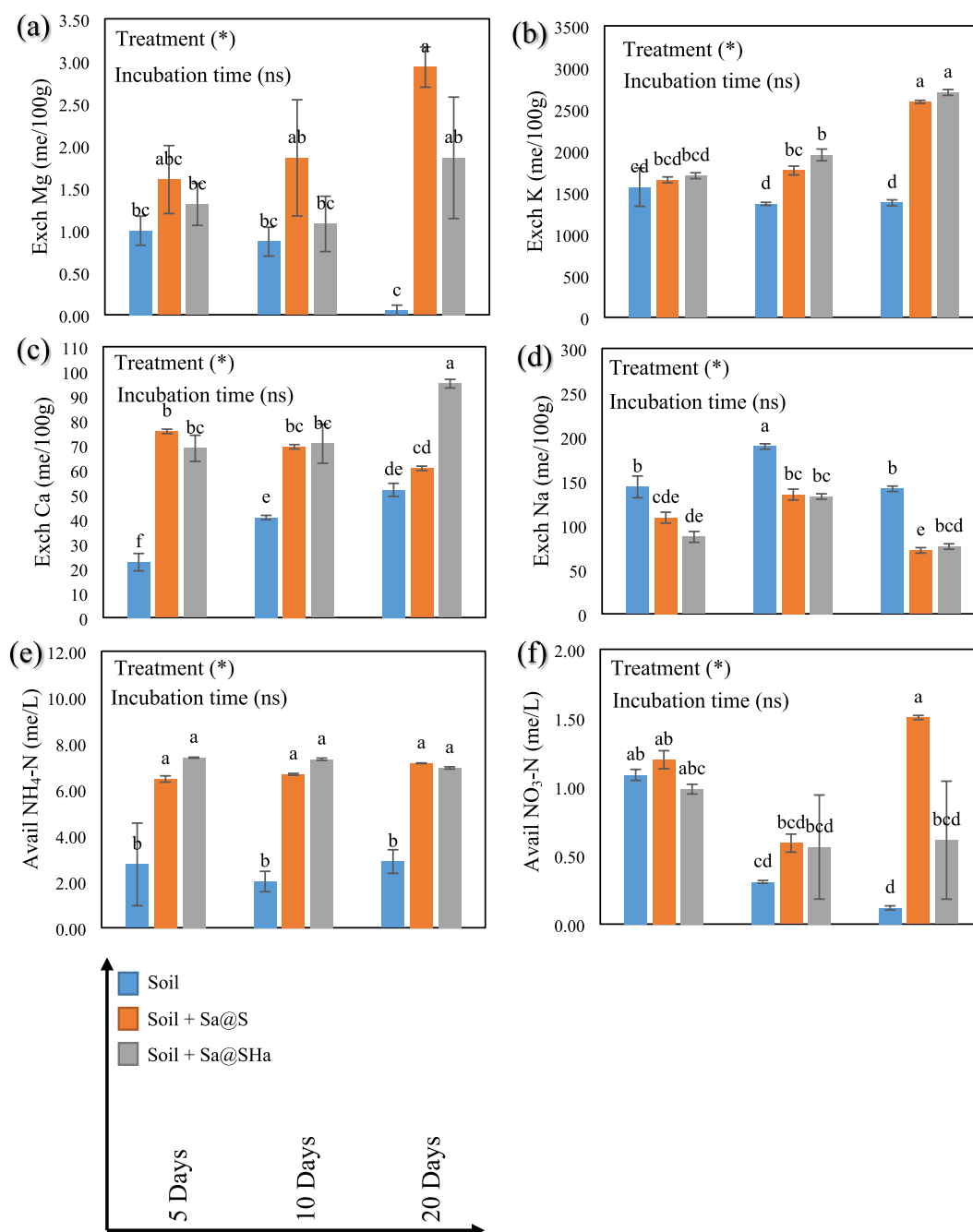


**Fig. 8.** Soil characteristics (Exchangeable Mg, K, Ca, Na, Available NH<sub>4</sub>-N, and NO<sub>3</sub>-N) in saline soil regarding hydrogel beads application at different incubation times. The vertical bars indicate the mean standard error. Avail: Available, Exch: Exchangeable. Control: soil only, Sa@S: soil + Sa@S samples, Sa@SHa: soil + Sa@SHa samples. Statistically significant at a significance level of  $P \leq 0.05$  in Tukey's test.

the following order: Sa@SHa > Sa@S > soil. This is because carboxyl (-COOH) and aromatic rings from polymer composites can attract and bind to positively charged cations. When these functional groups interact with soil particles, they create additional sites for cation adsorption, increasing CEC.

Fig. 8a-c depicts the exchangeable Mg, K, and Ca values for all treatments. The data shows that hydrogel beads encapsulated-struvite treatment leads to a significant increase in Mg, K and Ca ( $P \leq 0.05$ ) compared to the control. After 20 days of incubation, the Sa@S treatment exhibited the highest concentration of Mg, with a 99.31 % increase compared to the control, followed by the Sa@SHa treatment, with a 97.31 % increase. The Sa@SHa treatment also showed the highest concentration of K and Ca after 20 days of incubation, with 49.07 % and

46.87 % increases, respectively. These findings were due to the presence of struvite, a mineral complex of Mg and Ca ions, in the hydrogel beads. When these beads disintegrate into the soil, they release ions contributing to the soil's exchangeable Mg and Ca pools. Because of its porous nature, the hydrogel absorbed and retained significant water and nutrients such as K ion. Consequently, when these beads are added to the soil, they function as containers for K ion, thereby avoiding the leaching process and subsequent loss of nutrients (Hidayat et al., 2024b).

In contrast, the decrease in exchangeable Na was substantial ( $P \leq 0.05$ ) after treatment with hydrogel beads encapsulated (Fig. 8d). Specifically, there was a reduction of up to 48.93 % for Sa@S and 46.09 % for Sa@SHa. Lowering the Na concentration in soil can positively impact plant growth (Almeida et al., 2017; Kronzucker et al., 2013). This

finding agrees with the results of (Costa et al., 2022), who used a hydrogel composed of potassium acrylate and acrylamide to recover saline soil.

#### 3.4.4. Available $\text{NH}_4\text{-N}$ and $\text{NO}_3\text{-N}$

$\text{NH}_4\text{-N}$  and  $\text{NO}_3\text{-N}$  are essential forms of nitrogen in soil that are vital for plant growth and soil fertility (Xu et al., 2012). These forms of nitrogen are used by plants through their roots and utilized for various physiological processes (Hachiya et al., 2012; Zayed et al., 2023). The study showed a significant increase ( $P \leq 0.05$ ) in  $\text{NH}_4\text{-N}$  levels in the soil with treatment (Fig. 8e). After 20 days of incubation, the highest concentration of  $\text{NH}_4\text{-N}$  was observed in Sa@S with a 26.57 % increase, followed by Sa@SHa with an 18.52 % increase compared to the control. The increase observed over incubation time suggests the conversion of readily convertible nutrients to minerals. Additionally, the study discovered a significant increase ( $P \leq 0.05$ ) in  $\text{NO}_3\text{-N}$  concentration in soil samples incubated after the hydrogel beads encapsulated application (Fig. 8f). After 20 days of incubation,  $\text{NO}_3\text{-N}$  concentration increased by 92.15 % and 80.68 % for Sa@S and Sa@SHa, respectively. This result is similar to the findings of (Tefera et al., 2022), who reported that liquefied biomass hydrogel increased  $\text{NH}_4\text{-N}$  and  $\text{NO}_3\text{-N}$  values under saline soil conditions.

## 4. Conclusions

Soil salinity exerts a negative impact on crop productivity due to excessive nutrient levels in the soil. To address this issue, the efficacy of slow-release mineral fertilizers struvite encapsulated in hydrogel beads was investigated. In this study, a two-step process was employed to synthesize the hydrogel beads. Firstly, struvite was synthesized by mixing magnesium, ammonium-nitrogen, and phosphate in equal proportions. Secondly, hydrogel beads were formed using sodium alginate-poly (acrylic acid) and humic acid. Subsequently, the struvite was combined with the hydrogel beads to create Sa@S (without humic acid) and Sa@SHa (with humic acid). The findings revealed that the optimal conditions for struvite formation occurred at pH 9.0. The study on slow-release mineral fertilizers indicated a significant release of nutrients from struvite compared to encapsulated struvite hydrogel beads ( $P \leq 0.05$ ). Swelling experiments demonstrated that Sa@S exhibited higher water retention capacities compared to Sa@SHa. Additionally, experiments on soil water loss rate (SWL rate) confirmed the ability of hydrogel beads to retain water in the soil, reducing soil water loss by up to 33.33 % compared to intact soil. Furthermore, the soil salinity incubation experiment reveals a significant reduction in soil EC and Na after treatment with the hydrogel bead encapsulation. However, there is no considerable variation in pH and SOC. Additionally, there was a significant increase ( $P \leq 0.05$ ) in the available  $\text{NH}_4\text{-N}$ ,  $\text{NO}_3\text{-N}$ , P, CEC, and exchangeable Ca, Mg and K levels. These experiments suggest that the encapsulated struvite hydrogel beads efficiently reduce salts and improve soil properties.

## CRedit authorship contribution statement

**Endar Hidayat:** Writing – review & editing, Writing – original draft, Visualization, Validation, Methodology, Investigation, Formal analysis, Data curation, Conceptualization. **Nur Maisarah Mohamad Sarbani:** Writing – review & editing, Validation, Software. **Sadaki Samitsu:** Writing – review & editing, Visualization, Validation, Supervision, Resources. **Ferry Anggoro Ardy Nugroho:** Writing – review & editing, Validation. **Sudip Kumar Lahiri:** Writing – review & editing, Validation. **Mitsuru Aoyagi:** Supervision. **Seiichiro Yonemura:** Supervision. **Hiroyuki Harada:** Visualization, Supervision, Project administration, Funding acquisition.

## Declaration of competing interest

The authors declare that they have no known competing financial interests or personal relationships that could have appeared to influence the work reported in this paper.

## Acknowledgement

Endar Hidayat (E.H.) wishes to thank the MEXT Scholarship for providing sponsorship during studies at the Prefectural University of Hiroshima. E. H. would like to express gratitude to the National Institute for Materials Science (NIMS), Japan, for accepting the research internship.

## References

- Abd El-Aziz, M.E., Salama, D.M., Morsi, S.M.M., Youssef, A.M., El-Sakhawy, M., 2022. Development of polymer composites and encapsulation technology for slow-release fertilizers. *Rev. Chem. Eng.* 38, 603–616. <https://doi.org/10.1515/revce-2020-0044>.
- Abdeen, Z.U., Saeed, R., 2019. Soil desalination via poly(vinyl alcohol) borate hydrogel. *Theor. Found. Chem. Eng.* 53, 1094–1098. <https://doi.org/10.1134/S0040579519060010>.
- Abdel-Fattah, M.K., 2012. Role of gypsum and compost in reclaiming saline-sodic soils. *IOSR J. Agric. Vet. Sci.* 1, 30–38. <https://doi.org/10.9790/2380-0133038>.
- Ahamed, G.J., Li, X., Liu, A., Chen, S., 2020. Brassinosteroids in plant tolerance to abiotic stress. *J. Plant Growth Regul.* 39, 1451–1464. <https://doi.org/10.1007/s00344-020-10098-0>.
- Almeida, D.M., Oliveira, M.M., Saibo, N.J.M., 2017. Regulation of  $\text{Na}^+$  and  $\text{K}^+$  homeostasis in plants: towards improved salt stress tolerance in crop plants. *Genet. Mol. Biol.* 40, 326–345. <https://doi.org/10.1590/1678-4685-gmb-2016-0106>.
- Andrade Foronda, D., Colinet, G., 2023. Prediction of soil salinity/sodicity and salt-affected soil classes from soluble salt ions using machine learning algorithms. *Soil Syst* 7, 47. <https://doi.org/10.3390/soilsystems7020047>.
- Ashraf, M., Harris, P.J.C., 2004. Potential biochemical indicators of salinity tolerance in plants. *Plant Sci.* 166, 3–16. <https://doi.org/10.1016/j.plantsci.2003.10.024>.
- Atalay, S., Sargin, I., Arslan, G., 2022. Slow-release mineral fertilizer system with chitosan and oleic acid-coated struvite-K derived from pumpkin pulp. *Cellul.* 29, 2513–2523. <https://doi.org/10.1007/s10570-022-04453-5>.
- Bechtaoui, N., Rabiou, M.K., Raklami, A., Oufdou, K., Hafidi, M., Jemo, M., 2021. Phosphate-dependent regulation of growth and stresses management in plants. *Front. Plant Sci.* 12. <https://doi.org/10.3389/fpls.2021.679916>.
- Bogdan, A., O'Donnell, C., Robles Aguilar, A.A., Sigurnjak, I., Power, N., Michels, E., Harrington, J., Meers, E., 2021. Impact of time and phosphorus application rate on phosphorus bioavailability and efficiency of secondary fertilizers recovered from municipal wastewater. *Chemosphere* 282, 131017. <https://doi.org/10.1016/j.chemosphere.2021.131017>.
- Cevheri, C.I., Sakin, E., Ramazanoglu, E., 2022. Effects of different fertilizers on some soil enzymes activity and chlorophyll contents of two cotton (*G. hirsutum* L.) varieties grown in a saline and non-saline soil. *J. Plant Nutr.* 45, 95–106. <https://doi.org/10.1080/01904167.2021.1949467>.
- Chen, X., Kou, M., Tang, Z., Zhang, A., Li, H., Wei, M., 2017. Responses of root physiological characteristics and yield of sweet potato to humic acid urea fertilizer. *PLoS One* 12, e0189715. <https://doi.org/10.1371/journal.pone.0189715>.
- Chinthakuntla, A., Venkateswara Rao, K., Rao Kandregula, G., 2016. MgO Nanoparticles prepared by microwave-irradiation technique and its seed germination application. *Nano Trends A J. Nanotechnol. Appl.*
- Costa, M.C.G., Freire, A.G., Lourenço, D.V., de Sousa, R.R., de A. Feitosa, J.P., Mota, J.C.A., 2022. Hydrogel composed of potassium acrylate, acrylamide, and mineral as soil conditioner under saline conditions. *Sci. Agric.* 79. <https://doi.org/10.1590/1678-992x-2020-0235>.
- Das, D., Bhattacharjee, S., Bhaladhare, S., 2023. Preparation of cellulose hydrogels and hydrogel nanocomposites reinforced by crystalline cellulose nanofibers (CNFs) as a water reservoir for agriculture use. *ACS Appl. Polym. Mater.* 5, 2895–2904. <https://doi.org/10.1021/acscpm.3c00109>.
- de Oliveira, J.L., Campos, E.V.R., Camara, M.C., Della Vecchia, J.F., de Matos, S.T.S., de Andrade, D.J., Gonçalves, K.C., Nascimento, J., do Polanczyk, R.A., de Araújo, D.R., Fraceto, L.F., 2020. Hydrogels containing botanical repellents encapsulated in zein nanoparticles for crop protection. *ACS Appl. Nano Mater.* 3, 207–217. <https://doi.org/10.1021/acscan.9b01917>.
- Ding, X., Jiang, Y., Zhao, H., Guo, D., He, L., Liu, F., Zhou, Q., Nandwani, D., Hui, D., Yu, J., 2018. Electrical conductivity of nutrient solution influenced photosynthesis, quality, and antioxidant enzyme activity of pakchoi (*Brassica campestris* L. ssp. *Chinensis*) in a hydroponic system. *PLoS One* 13, e0202090. <https://doi.org/10.1371/journal.pone.0202090>.
- Ding, Y., Zhang, G., Wu, H., Hai, B., Wang, L., Qian, Y., 2001. Nanoscale magnesium hydroxide and magnesium oxide powders: control over size, shape, and structure via hydrothermal synthesis. *Chem. Mater.* 13, 435–440. <https://doi.org/10.1021/cm000607e>.
- Elrashidi, M.A., West, L.T., Seybold, C.A., Benham, E.C., Schoeneberger, P.J., Ferguson, R., 2010. Effects of gypsum addition on solubility of nutrients in soil

- amended with peat. *Soil Sci.* 175, 162–172. <https://doi.org/10.1097/SS.0b013e3181dd51d0>.
- Ennab, H.A., Mohamed, A.H., El-Hoseiny, H.M., Omar, A.A., Hassan, I.F., Gaballah, M.S., Khalil, S.E., Mira, A.M., Abd El-Khalek, A.F., Alam-Eldein, S.M., 2023. Humic acid improves the resilience to salinity stress of drip-irrigated mexican lime trees in saline clay soils. *Agronomy* 13, 1680. <https://doi.org/10.3390/agronomy13071680>.
- Fageria, N.K., Moreira, A., Moraes, L.A.C., Moraes, M.F., 2014. Influence of lime and gypsum on yield and yield components of soybean and changes in soil chemical properties. *Commun. Soil Sci. Plant Anal.* 45, 271–283. <https://doi.org/10.1080/00103624.2013.861906>.
- Faturechi, R., Karimi, A., Hashemi, A., Yousefi, H., Navidbakhsh, M., 2015. Influence of Poly(acrylic acid) on the mechanical properties of composite hydrogels. *Adv. Polym. Tech.* 34 <https://doi.org/10.1002/adv.21487>.
- Gharaibeh, M.A., Albalasmeh, A.A., Pratt, C., El Hanandeh, A., 2021. Estimation of exchangeable sodium percentage from sodium adsorption ratio of salt-affected soils using traditional and dilution extracts, saturation percentage, electrical conductivity, and generalized regression neural networks. *Catena (amst)* 205, 105466. <https://doi.org/10.1016/j.catena.2021.105466>.
- González-Morales, C., Fernández, B., Molina, F.J., Naranjo-Fernández, D., Matamoros-Veloz, A., Camargo-Valero, M.A., 2021. Influence of pH and temperature on struvite purity and recovery from anaerobic digestate. *Sustainability* 13, 10730. <https://doi.org/10.3390/su131910730>.
- Grzyb, A., Wolna-Maruwka, A., Niewiadomska, A., 2020. Environmental factors affecting the mineralization of crop residues. *Agronomy* 10, 1951. <https://doi.org/10.3390/agronomy10121951>.
- Hachiya, T., Watanabe, C.K., Fujimoto, M., Ishikawa, T., Takahara, K., Kawai-Yamada, M., Uchimiya, H., Uesono, Y., Terashima, I., Noguchi, K., 2012. Nitrate addition alleviates ammonium toxicity without lessening ammonium accumulation, organic acid depletion and inorganic cation depletion in arabisopsis thaliana shoots. *Plant Cell Physiol.* 53, 577–591. <https://doi.org/10.1093/pcp/pcs012>.
- Hidayat, E., Mohamad Sarbani, N.M.B., Yonemura, S., Mitoma, Y., Harada, H., 2023. Application of box-behnken design to optimize phosphate adsorption conditions from water onto novel adsorbent CS-ZL/ZrO/Fe3O4: characterization, equilibrium, isotherm, kinetic, and desorption studies. *Int. J. Mol. Sci.* 24 <https://doi.org/10.3390/ijms241119754>.
- Hidayat, E., Sarbani, N.M.M., Susanto, H.B., Situngkir, Y.V., Chrisandi, M.W., Samitsu, S., Mitoma, Y., Yonemura, S., Harada, H., 2024a. Performance of hydrogel beads composites derived from sodium alginate-cetyltrimethylammonium bromide toward congo red dye adsorption from aqueous solution. *Desalination Water Treat.* 100313. <https://doi.org/10.1016/j.dwt.2024.100313>.
- Hidayat, E., Sarbani, N.M.M., Lahiri, S.K., Samitsu, S., Yonemura, S., Mitoma, Y., Harada, H., 2024b. Effects of sodium alginate-poly(acrylic acid) cross-linked hydrogel beads on soil conditioner in the absence and presence of phosphate and carbonate ions. *Case Studies in Chemical and Environ. Eng.* 9, 100642 <https://doi.org/10.1016/j.csee.2024.100642>.
- Hua, S., Ma, H., Li, X., Yang, H., Wang, A., 2010. pH-sensitive sodium alginate/poly(vinyl alcohol) hydrogel beads prepared by combined Ca<sup>2+</sup> crosslinking and freeze-thawing cycles for controlled release of diclofenac sodium. *Int. J. Biol. Macromol.* 46, 517–523. <https://doi.org/10.1016/j.ijbiomac.2010.03.004>.
- Jamir, E., Kangabam, R., Das, Borah, K., Tamuly, A., Deka Boruah, H.P., Silla, Y., (2019). Role of Soil Microbiome and Enzyme Activities in Plant Growth Nutrition and Ecological Restoration of Soil Health. pp. 99–132. DOI: 10.1007/978-981-13-9117-0.5.
- Kronzucker, H.J., Coskun, D., Schulze, L.M., Wong, J.R., Britto, D.T., 2013. Sodium as nutrient and toxicant. *Plant and Soil* 369, 1–23. <https://doi.org/10.1007/s11104-013-1801-2>.
- Kumar, P., Sharma, P.K., 2020. Soil Salinity and Food Security in India. *Front Sustain Food Syst.* 4 <https://doi.org/10.3389/fsufs.2020.533781>.
- Leogrande, R., Vitti, C., 2019. Use of organic amendments to reclaim saline and sodic soils: a review. *Arid Land Res. Manag.* 33, 1–21. <https://doi.org/10.1080/15324982.2018.1498038>.
- Li, Y., Fang, F., Wei, J., Wu, X., Cui, R., Li, G., Zheng, F., Tan, D., 2019. Humic acid fertilizer improved soil properties and soil microbial diversity of continuous cropping peanut: a three-year experiment. *Sci. Rep.* 9, 12014. <https://doi.org/10.1038/s41598-019-48620-4>.
- Li, Z., Zhang, M., 2023. Progress in the preparation of stimulus-responsive cellulose hydrogels and their application in slow-release fertilizers. *Polymers (Basel)* 15, 3643. <https://doi.org/10.3390/polym15173643>.
- Liang, X.Q., Chen, Y.X., Li, H., Tian, G.M., Ni, W.Z., He, M.M., Zhang, Z.J., 2007. Modeling transport and fate of nitrogen from urea applied to a near-trench paddy field. *Environ. Pollut.* 150, 313–320. <https://doi.org/10.1016/j.envpol.2007.02.003>.
- Liang, J., Li, Y., Si, B., Wang, Y., Chen, X., Wang, X., Chen, H., Wang, H., Zhang, F., Bai, Y., Biswas, A., 2021. Optimizing biochar application to improve soil physical and hydraulic properties in saline-alkali soils. *Sci. Total Environ.* 771, 144802 <https://doi.org/10.1016/j.scitotenv.2020.144802>.
- Malcolm, B.J., Cameron, K.C., Curtin, D., Di, H.J., Beare, M.H., Johnstone, P.R., Edwards, G.R., 2019. Organic matter amendments to soil can reduce nitrate leaching losses from livestock urine under simulated fodder beet grazing. *Agr. Ecosyst Environ* 272, 10–18. <https://doi.org/10.1016/j.agee.2018.11.003>.
- Metternicht, G.I., Zinck, J.A., 2003. Remote sensing of soil salinity: potentials and constraints. *Remote Sens. Environ.* 85, 1–20. [https://doi.org/10.1016/S0034-4257\(02\)00188-8](https://doi.org/10.1016/S0034-4257(02)00188-8).
- Moreira, A., Sfredo, G.J., Moraes, L.A.C., Fageria, N.K., 2015. Lime and cattle manure in soil fertility and soybean grain yield cultivated in tropical soil. *Commun. Soil Sci. Plant Anal.* 46, 1157–1169. <https://doi.org/10.1080/00103624.2015.1033542>.
- Munns, R., Passioura, J.B., Colmer, T.D., Byrt, C.S., 2020. Osmotic adjustment and energy limitations to plant growth in saline soil. *New Phytol.* 225, 1091–1096. <https://doi.org/10.1111/nph.15862>.
- Negacz, K., Malek, Z., de Vos, A., Vellinga, P., 2022. Saline soils worldwide: Identifying the most promising areas for saline agriculture. *J. Arid Environ.* 203 <https://doi.org/10.1016/j.jaridenv.2022.104775>.
- Niu, Y., Ke, R., Yang, T., Song, J., 2020. pH-responsively water-retaining controlled-release fertilizer using humic acid hydrogel and nano-silica aqueous dispersion. *J. Nanosci. Nanotechnol.* 20, 2286–2291. <https://doi.org/10.1166/jnn.2020.17216>.
- Nörnberg, A.B., Gehrke, V.R., Mota, H.P., Camargo, E.R., Fajardo, A.R., 2019. Alginate-cellulose biopolymeric beads as efficient vehicles for encapsulation and slow-release of herbicide. *Colloids Surf A Physicochem Eng Asp* 583, 123970. <https://doi.org/10.1016/j.colsurfa.2019.123970>.
- Olad, A., Zebhi, H., Salari, D., Mirmohseni, A., Reyhani Tabar, A., 2018. Slow-release NPK fertilizer encapsulated by carboxymethyl cellulose-based nanocomposite with the function of water retention in soil. *Mater. Sci. Eng. C* 90, 333–340. <https://doi.org/10.1016/j.msec.2018.04.083>.
- Qadir, A., Khan, S.A., Ahmad, R., Masood, S., Irshad, M., Kaleem, F., Kumar, S., Shahzad, M., 2017. Exogenous Ca 2 SiO 4 enrichment reduces the leaf apoplastic Na + and increases the growth of okra (*Abelmoschus esculentus* L.) under salt stress. *Sci. Hortic.* 214, 1–8. <https://doi.org/10.1016/j.scienta.2016.11.008>.
- Qiao, D., Liu, H., Yu, L., Bao, X., Simon, G.P., Petinakis, E., Chen, L., 2016. Preparation and characterization of slow-release fertilizer encapsulated by starch-based superabsorbent polymer. *Carbohydr. Polym.* 147, 146–154. <https://doi.org/10.1016/j.carbpol.2016.04.010>.
- Rabat, N.E., Hashim, S., Majid, R.A., 2016. Effect of Different Monomers on Water Retention Properties of Slow Release Fertilizer Hydrogel. *Procedia Engineering.* Elsevier Ltd, in pp. 201–207.
- Rashid, M.I., Mujawar, L.H., Shahzad, T., Almeelbi, T., Ismail, I.M.I., Oves, M., 2016. Bacteria and fungi can contribute to nutrients bioavailability and aggregate formation in degraded soils. *Microbiol. Res.* 183, 26–41. <https://doi.org/10.1016/j.micres.2015.11.007>.
- Razzaghi, F., Arthur, E., Moosavi, A.A., 2021. Evaluating models to estimate cation exchange capacity of calcareous soils. *Geoderma* 400, 115221. <https://doi.org/10.1016/j.geoderma.2021.115221>.
- Rech, I., Withers, P., Jones, D., Pavinato, P., 2018. Solubility, diffusion and crop uptake of phosphorus in three different struvites. *Sustainability* 11, 134. <https://doi.org/10.3390/su11010134>.
- Satheesh Kumar, K.V., Bindu, M., Suresh, S., Anil, A., Sujoy, S., Mohanan, A., Periyat, P., 2023. Investigation on swelling behavior of sodium alginate/black titania nanocomposite hydrogels and effect of synthesis conditions on water uptake. *Results in Eng.* 20, 101460 <https://doi.org/10.1016/j.rineng.2023.101460>.
- Shahid, S.A., Zaman, M., Heng, L., 2018. Introduction to soil salinity, sodicity and diagnostics techniques, in: guideline for salinity assessment, mitigation and adaptation using nuclear and related techniques. Springer Int. Publishing, Cham. 1–42. [https://doi.org/10.1007/978-3-319-96190-3\\_1](https://doi.org/10.1007/978-3-319-96190-3_1).
- Shirokova, Y., Forkutsa, I., Sharafutdinova, N., 2000. Use of electrical conductivity instead of soluble salts for soil salinity monitoring in central Asia. *Irrig. Drain. Syst. Irrigation and Drainage Systems* 14, 199–206. <https://doi.org/10.1023/A:1026560204665>.
- Shrivastava, P., Kumar, R., 2015. Soil salinity: a serious environmental issue and plant growth promoting bacteria as one of the tools for its alleviation. *Saudi J. Biol. Sci.* 22, 123–131. <https://doi.org/10.1016/j.sjbs.2014.12.001>.
- Tanehgonbadi, M., Qaderi, F., 2023. Investigation of the effect of initial composition of soil on the efficiency of desalination by polyvinyl alcohol borate hydrogel. *Environ. Earth Sci.* 82, 340. <https://doi.org/10.1007/s12665-023-11009-8>.
- Tefera, B.B., Bayabil, H.K., Tong, Z., Teshome, F.T., Wenbo, P., Li, Y.C., Hailegnaw, N.S., Gao, B., 2022. Using liquefied biomass hydrogel to mitigate salinity in salt-affected soils. *Chemosphere* 309, 136480. <https://doi.org/10.1016/j.chemosphere.2022.136480>.
- Valle, S.F., Giroto, A.S., Dombin, V., Robles-Aguilar, A.A., Jablonowski, N.D., Ribeiro, C., 2022. Struvite-based composites for slow-release fertilization: a case study in sand. *Sci. Rep.* 12 <https://doi.org/10.1038/s41598-022-18214-8>.
- Venezia, V., Avallone, P.R., Vitiello, G., Silvestri, B., Grizzuti, N., Pasquino, R., Luciani, G., 2022. Adding humic acids to gelatin hydrogels: a way to tune gelation. *Biomacromolecules* 23, 443–453. <https://doi.org/10.1021/acs.biomac.1c01398>.
- Victor Roch, G., Maharajan, T., Ceasar, S.A., Ignacimuthu, S., 2019. The role of PHT1 family transporters in the acquisition and redistribution of phosphorus in plants. *CRC Crit. Rev. Plant Sci.* 38, 171–198. <https://doi.org/10.1080/07352689.2019.1645402>.
- Wang, L., Ye, C., Gao, B., Wang, X., Li, Y., Ding, K., Li, H., Ren, K., Chen, S., Wang, W., Ye, X., 2023. Applying struvite as a N-fertilizer to mitigate N2O emissions in agriculture: feasibility and mechanism. *J. Environ. Manage.* 330, 117143 <https://doi.org/10.1016/j.jenvman.2022.117143>.
- Xu, G., Fan, X., Miller, A.J., 2012. Plant nitrogen assimilation and use efficiency. *Annu. Rev. Plant Biol.* 63, 153–182. <https://doi.org/10.1146/annurev-arplant-042811-105532>.
- Zahedifar, M., 2020. Effect of biochar on cadmium fractions in some polluted saline and sodic soils. *Environ. Manag.* 66, 1133–1141. <https://doi.org/10.1007/s00267-020-01371-9>.
- Zayed, O., Hewedy, O.A., Abdelmoteleb, A., Ali, M., Youssef, M.S., Roumia, A.F., Seymour, D., Yuan, Z.-C., 2023. Nitrogen journey in plants: from uptake to metabolism, stress response, and microbe interaction. *Biomolecules* 13, 1443. <https://doi.org/10.3390/biom13101443>.

- Zhang, Y.-Y., Wu, W., Liu, H., 2019. Factors affecting variations of soil pH in different horizons in hilly regions. *PLoS One* 14, e0218563. <https://doi.org/10.1371/journal.pone.0218563>.
- Zhang, Y., Yang, J., Yao, R., Wang, X., Xie, W., 2020. Short-term effects of biochar and gypsum on soil hydraulic properties and sodicity in a saline-alkali soil. *Pedosphere* 30, 694–702. [https://doi.org/10.1016/S1002-0160\(18\)60051-7](https://doi.org/10.1016/S1002-0160(18)60051-7).
- Zhao, C., Zhang, H., Song, C., Zhu, J.-K., Shabala, S., 2020. Mechanisms of plant responses and adaptation to soil salinity. *The Innovation* 1, 100017. <https://doi.org/10.1016/j.xinn.2020.100017>.
- Zhou, X., Chen, Y., 2019. An integrated process for struvite electrochemical precipitation and ammonia oxidation of sludge alkaline hydrolysis supernatant. *Environ. Sci. Pollut. Res.* 26, 2435–2444. <https://doi.org/10.1007/s11356-018-3667-6>.